In Vivo Feasibility of Real-Time Monitoring of Focused Ultrasound Surgery (FUS) Using Harmonic Motion Imaging (HMI)

Caroline Maleke, *Student Member, IEEE*, and Elisa E. Konofagou*, *Member, IEEE*

***Abstract*—In this study, the Harmonic Motion Imaging for Focused Ultrasound (HMIFU) technique is applied to monitor changes in mechanical properties of tissues during thermal therapy in a transgenic breast cancer mouse model *in vivo*. An HMIFU system, composed of a 4.5-MHz focused ultrasound (FUS) and a 3.3-MHz phased-array imaging transducer, was mechanically moved to image and ablate the entire tumor. The FUS transducer was driven by an amplitude-modulated (AM) signal at 15 Hz. The acoustic intensity (I_{spta}) was equal to 1050 W/cm^2 at the focus. A digital low-pass filter was used to filter out the spectrum of the FUS beam and its harmonics prior to displacement estimation. The resulting axial displacement was estimated using 1-D cross-correlation on the acquired RF signals. Results from two mice with eight lesions formed in each mouse (16 lesions total) showed that the average peak-to-peak displacement amplitude before and after lesion formation was respectively equal to 17.34 $\pm$ 1.34 μm and 10.98 $\pm$ 1.82 μm ($p < 0.001$). Cell death was also confirmed by hematoxylin and eosin histology. HMI displacement can be used to monitor the relative tissue stiffness changes in real time during heating so that the treatment procedure can be performed in a time-efficient manner. The HMIFU system may, therefore, constitute a cost-efficient and reliable alternative for real-time monitoring of thermal ablation.**

***Index Terms*—Acoustic radiation force, breast cancer, focused ultrasound surgery (FUS), harmonic motion imaging, high-intensity focused ultrasound (HIFU), *in vivo*, monitoring, noninvasive estimation, tissue ablation, ultrasound.**

I. Introduction

THE POTENTIAL of focused ultrasound surgery (FUS) as a noninvasive modality for cancer treatment has become a promising approach in recent years [1]. FUS produces an acoustic wave that propagates through tissue and deposits high acoustic energy only at the localized focus of the transducer. High acoustic energy at the localized focus results in rapid temperature elevation that causes cellular death (coagulation necrosis) in tissues (i.e., thermal lesions), while the surrounding tissues remain relatively intact.

The limitations of FUS mainly lie in the difficulty in monitoring temperature rise and controlling the desired volume of tissue necrosis at the ablation site. MRI has been used for noninvasive guidance and monitoring of thermal therapies, because it can offer quantitative spatial maps of the temperature rise at high spatial resolution [2]–[4]. This technique is also known as MR-guided FUS [3], [5]–[9]. However, the FUS technique is in itself a low-cost treatment technique that currently requires a costly monitoring device, i.e., an MRI system.

Several techniques have been developed to monitor the formation of lesions during FUS surgery based on the underlying tissue stiffness [9]–[12]. It has been shown that tissue stiffness decreases (or, displacement increases) at the beginning of heating, and, if the heating is sustained beyond a threshold temperature, irreversible changes occur. The tissue stiffness then increases (or, displacement decreases) nonlinearly, which indicates that a lesion has been formed due to heat-induced structural and mechanical changes in the tissue [9], [10], [13], [14].

Our objective is to develop a low-cost, real-time monitoring technique of tissue mechanical changes during thermal therapy with a precise and optimal treatment time (thermal dose) and controlled lesion size. Previously, we introduced an all-ultrasound-based system for both ablation and imaging, namely, Harmonic Motion Imaging for Focused Ultrasound (HMIFU) [13]. Here, the HMIFU system was further improved by utilizing a phased-array imaging transducer to replace the previously used single-element pulse-echo transducer and to provide a 2-D view of the targeted region (see Fig. 1). HMI is a radiation-force-based technique that induces vibration at the focal zone of an FUS transducer for the detection of localized stiffness changes [13]. An amplitude-modulated (AM) signal was used to generate the harmonic radiation force in a specific region by a single-element FUS transducer. An AM beam

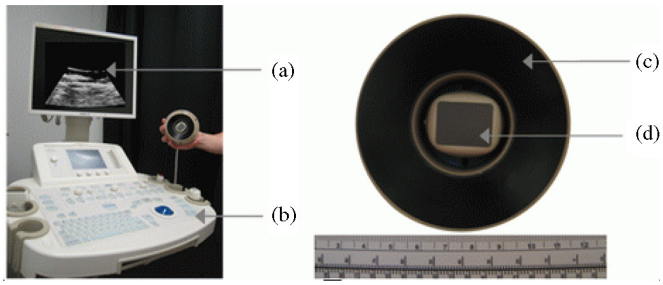

Fig. 1. (a) Two-dimensional B-mode image during ablation and (b) the console of the Sonix RP system used. The HMIFU transducer consists of a single-element FUS transducer with a center frequency of: (c) 4.5 MHz and (d) a 3.3-MHz phased-array imaging transducer.

Manuscript received April 20, 2009; revised June 24, 2009. First published July 28, 2009; current version published January 4, 2010. This work was supported by the National Institutes of Health under Grant R21EB008521. *Asterisk indicates corresponding author.*

C. Maleke is with the Department of Biomedical Engineering, Columbia University, New York, NY 10027 USA (e-mail: cm2243@columbia.edu).

*E. E. Konofagou is with the Department of Biomedical Engineering and Radiology, Columbia University, New York, NY 10027 USA (e-mail: ek2191@columbia.edu).

Color versions of one or more of the figures in this paper are available online at http://ieeexplore.ieee.org.

Digital Object Identifier 10.1109/TBME.2009.2027423

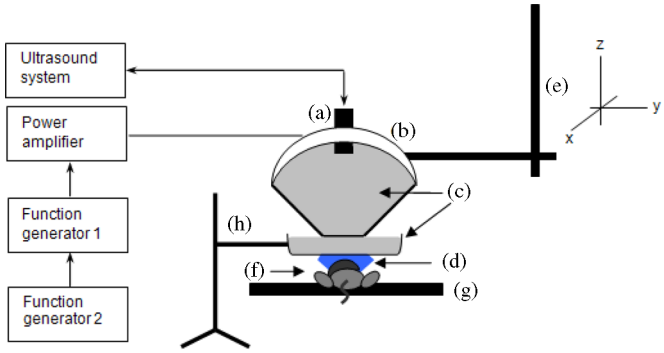

Fig. 2. Block diagram and schematic of the experimental HMIFU setup. (a) Phased-array imaging transducer, (b) FUS transducer, (c) degassed water, and (d) degassed ultrasound gel. HMIFU system was mounted on (e) the computer-controlled positioner. (f) Mouse was placed on (g) a heating platform (g). (h) Ring stand was used to hold the water chamber.

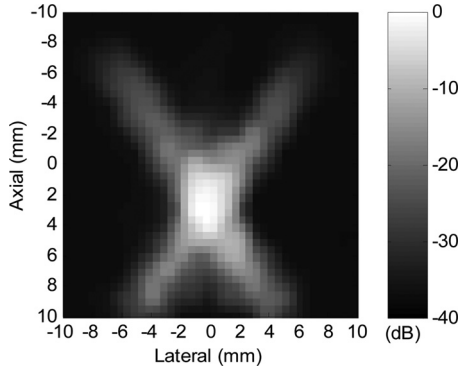

Fig. 3. Experimental beam profile of 4.5-MHz FUS transducer. The scale bar denotes the normalized acoustic intensity in dB relative to its peak at the focus.

offered an application of the radiation force at a stationary focus within the tissue region and a simpler transducer design [15].

One major advantage of this technique is that the resulting tissue displacements are imaged during the application of the acoustic radiation force, i.e., in their active mode, very similar to standard mechanical testing for the measurement of biomechanical properties [16]. The purpose of this study is to demonstrate the feasibility of HMIFU for real-time monitoring of tissue mechanical property changes during thermal therapy of tumors *in vivo*.

II. Methods

A. Experimental Setup

In vivo experiments were performed on two mice with mammary tumors (female, average weight of 32 $\pm$ 2 g), carrying conditional alleles for Brca1, Brca2, Bard1, and p53. A single mammary tumor mass developed in each mouse. The mammary tumors were invasive adenocarcinomas that formed bulky, round, solid regions, invading the surrounding fat and underlying pectoral muscle [17]. These mammary tumors can have high metastatic potential and typically grow up to 3–10 mm in diameter. The reader is prompted to Ludwig *et al.* [18] and Shakya *et al.* [17] for further details in the development of the transgenic mouse model used in this study.

The experimental setup is shown in Fig. 2. A 4.5-MHz FUS transducer [see Fig. 2(b); Imasonic, Voray-sur-l'Ognon, France] with a focal length of 45 $\pm$ 2 mm was used to generate the acoustic radiation force, using a low-frequency (AM) RF waveform. A function generator (Agilent/HP 33120A, Palo Alto, CA) was first used to produce the RF waveform at 4.5 MHz. Its amplitude was then modulated using a second function generator (Agilent 33220A, Palo Alto, CA) that generated a low frequency modulation at 15 Hz. The AM signal was amplified by 50 dB, using a power amplifier. The acoustic intensity (I_{spta}) at the focus was equal to 1050 W/cm^2. The duration of exposure to generate each lesion was equal to 13.5 s. To cover the entire tumor volume, several lesions were generated sequentially in a circular pattern by mechanically moving the transducer in 3-D, using a computer-controlled positioner [see Fig. 2(e)].

A phased-array imaging transducer of the Sonix RP system [see Fig. 2(a); Ultrasonix Medical Corporation, Richmond, Canada] with a center frequency of 3.3 MHz and bandwidth of 60% was inserted through a central opening of the FUS transducer; hence the beams of the two transducers were aligned [see Fig. 1(c) and (d)]. The consecutive RF frames were acquired at a sampling frequency of 40 MHz and a frame rate of 234 frames/s. Each frame was formed using a 36° field-of-view, a beam density of 1.78 beams/°, i.e., 64 beams per frame, a beamwidth of 2 mm, and a beam spacing of 1.12 mm at the focal depth (45 mm). A digital low-pass filter with a cutoff frequency of 4.2 MHz was applied on the acquired RF ultrasonic signals in order to filter out the FUS beam interference, prior to displacement estimation. A cross-correlation method was used to estimate the resulting axial displacements with the first frame as the reference. The correlation window used was equal to 1 mm with 87% overlap. The speed-of-sound changes as a result of heating can be simultaneously detected due to the associated linear shift in the estimated displacements [13]. To quantitatively compare the relative tissue stiffness before and after lesion formation, the speed of sound effect (i.e., the slope) was removed prior to analysis. The average data processing time for 234 HMI frames was equal to 1.8 min.

A 0.2-mm needle hydrophone (Precision Acoustics Ltd., Dorchester, U.K.) was used to measure the dimensions of the FUS beam. The needle hydrophone was mechanically moved in 2-D, i.e., 10 mm in the axial and 10 mm in the lateral direction, at a step size of 1 mm. The measured acoustic intensity profile of the FUS beam is shown in Fig. 3. The beam has an ellipsoidal shape with a major axis of 2 $\pm$ 0.5 mm and an orthogonal minor axis of 1 $\pm$ 0.5 mm (see Fig. 3).

B. Animal Preparation

All animal experimental procedures were approved by the Columbia University Institutional Animal Care and Use Committee. The experimental procedure was as follows: 1) the mice were anesthetized with isoflurane (1–5% mixture with 100% oxygen), and their pectoral areas were depilated; 2) the mice were placed on a heating platform (THM100, Indus

Instruments, Houston, TX) to maintain constant body temperature [see Fig. 2(f) and (g)]; 3) the FUS transducer was positioned over the tumor without requiring the animal to be submerged underwater. A water chamber was placed over the animal's chest to provide adequate matching and to maintain a normal body temperature in case thermal effects were experienced at the skin level [see Fig. 2(c)]. The water chamber was supported by a circular clamp, which was attached to a ring stand in order to keep the clamp stable and avoid any chest compression. There was a clearance of about 10 $\pm$ 2 mm between the bottom of the water chamber and the skin. Degassed ultrasound coupling gel was placed to ensure coupling in that area [see Fig. 2(d)]. The water chamber did not obstruct the normal respiratory patterns of the mice. The water chamber was kept at standard room temperature, i.e., between 20 °C and 25 °C; 4) the transducer was moved using a raster-scanning method [see Fig. 2(e)] at a step size of 1 mm until the entire tumor volume (approximately 200–500 mm^3) was ablated. The total treatment lasted approximately 30 min and depended on the tumor volume. There were eight lesions generated in each mouse, i.e., a total of 16 lesions for the two tumors studied.

C. Pathology

The mice were euthanized within 24 h of sonication, and the mammary tumors were subsequently excised. The specimens (untreated and treated tumors) were kept in 10% phosphate-buffered formalin (pH = 7) at low temperature (4 °C) for at least 24 h. The specimens were then rinsed in distilled water for 10 min, immersed in 70% isopropanol, and immediately submitted for pathology analysis. Tissue blocks were sampled from the central and peripheral edges of the treated tumor area and surrounding untreated mammary tumor for assessing the effect of FUS ablation. The specimens were embedded in paraffin, cut in 5-μm-thick slices, and stained with hematoxylin and eosin (H&E).

III. Results

Fig. 4 displays an example of grayscale B-mode images overlaid with color-coded peak-to-peak displacement amplitudes before and after lesion formation. The targeted tumor region is delineated in red [see Fig. 4(a)]. The focal region of the FUS beam is located at the center (0 mm) and at a depth of 45 $\pm$ 2 mm. The average displacement amplitude at the focal zone was approximately equal to 18 μm [see Fig. 4(a); in orange–red] and after the lesion was formed, the amplitude decreased to approximately 8 μm [see Fig. 4(b); in cyan]. Assuming uniform application of the radiation force, the resulting tissue motion (or, oscillatory displacement) can be related to the underlying relative tissue stiffness, and thus, to the stiffness change during heating. This motion can be visualized and quantified on the HMI M-mode images (see Fig. 5).

The image of the tissue motion was generated along the symmetry axis of the B-mode image (dashed line in Fig. 4(a)) over consecutive frames in time. Fig. 5 shows an example of the HMI M-mode images of the tumor region of approximately 8 mm in diameter with overlaid HMI oscillatory displacement

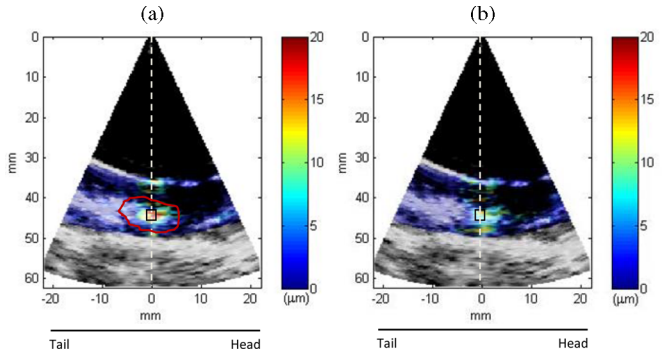

Fig. 4. Grayscale B-mode images of mammary tumor during heating *in vivo*. Colorbars denote peak-to-peak displacement amplitudes in μm. (a) Beginning of heating and (b) after lesion was formed. Red contour shows the targeted region (mammary tumor). For quantitative measurements, displacement amplitudes were averaged over a 3×3 mm^2 region (square). Dashed white line denotes a central RF line.

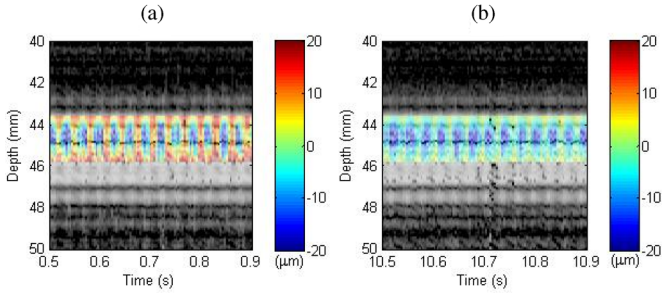

Fig. 5. Grayscale M-mode image of the tumor region with overlaid color-coded HMI displacements during heating. Colorbars denote displacement amplitude in μm. (a) At the beginning of heating (between 0.5 and 0.9 s) and (b) after lesion formation (between 10.5 and 10.9 s).

(see Fig. 5). The oscillatory displacement was estimated with respect to the initial frame. Tissue motion during heating is visible through the variation in displacement amplitude, which is denoted by alternating orange and blue in Fig. 5(a) or, light green and blue in Fig. 5(b). In orange (or, light green) the motion moving toward the transducer, and in blue represents the motion moving away from the transducer are denoted. Fig. 5(a) shows that, at the focal region, i.e., a depth of 45 $\pm$ 2 mm, the tumor tissue was initially displaced by at least twice the motion in Fig. 5(a) than that after lesion formation (Fig. 5(b)). Notice that the size of the displaced tissue at the focal region is approximately 2 mm in length, which is well correlated with the axial focal spot size of the FUS beam (2 $\pm$ 0.5 mm). Monitoring the displacement variation over time (see Fig. 6) confirmed that the tissue was coagulated after 10.5 s of heating [see Fig. 5(b)].

In order to quantitatively analyze the relative tissue stiffness change during heating, the resulting displacement around the focal region was then averaged over a 3 × 3 mm^2 region [see Fig. 4(a)] and plotted in time (see Fig. 6). The high periodic peaks in Fig. 6 correspond to the animal's chest movement as a result of respiration. The respiratory rate was approximately 38 breaths/min. This respiratory motion thus mainly remained along the axial direction since the animal was in the supine position (see Fig. 2) and had an average amplitude of 15 $\pm$ 2 μm. The entire respiratory motion thus remained within the

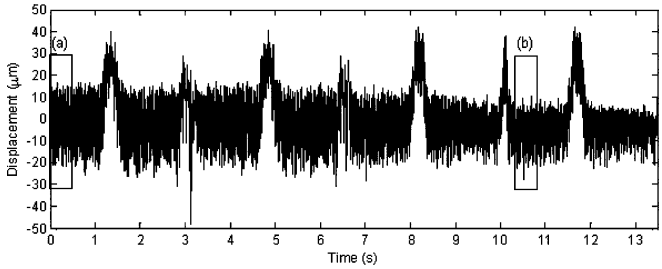

Fig. 6. HMI displacement variation during heating *in vivo*. The duration of exposure was approximately 13.5 s. The peaks indicate the respiratory motion of the mice during anesthesia. The respiratory rate was approximately 38 breaths/min. The magnification of displacement in regions (a) and (b) are shown in Fig. 7.

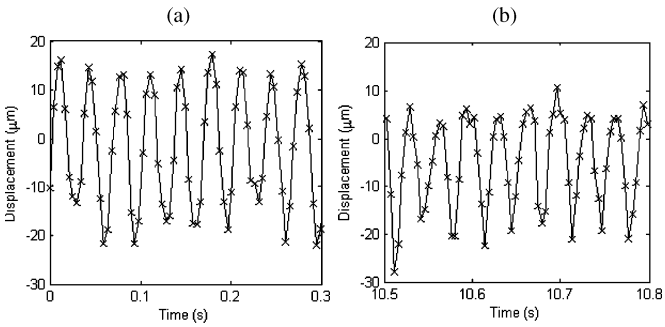

Fig. 7. HMI displacement within the selections in Fig. 6(a) and (b), i.e., at (a) 0–0.3 s and (b) 10.5–10.8 s of heating, respectively.

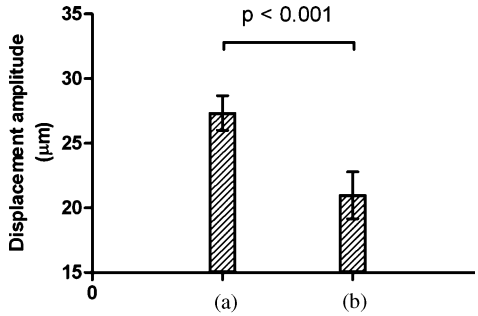

Fig. 8. Average peak-to-peak HMI displacement amplitudes from in two mice, i.e., 16 lesions total, (a) before lesion formation (between 0 and 6.5 s); mean = 27.34 μm, SD = 1.34, and (b) after lesion formation (between 6.6 and 13.5 s); mean = 20.98 μm, SD = 1.82. There is a statistically significant difference in HMI displacement amplitude before and after lesions were formed ($p < 0.001$).

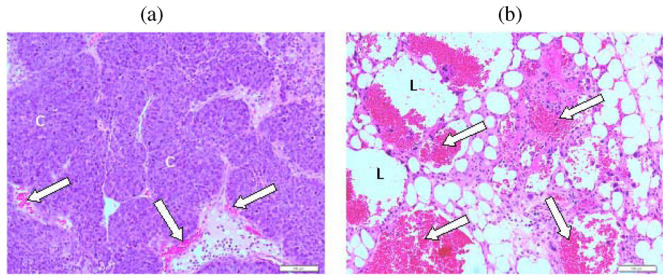

Fig. 9. Histology images with 100× magnification. Scale bar = 100 μm. (a) Nonablated tumor cells (= C); white arrows denote erythrocytes (red blood cells). (b) Ablated mammary tumors; damaged and necrotic cells indicated by hemorrhagic regions (white arrows) and fine fibrous strands outlined by adipose tissue (white lobes, *L*).

FUS focal region, i.e., 1 mm (axial) × 2 mm (lateral), and did not affect the location of the lesion within the tumor region. The tumors were ablated in a well-delineated zone of tissue, which was approximately 5–10 mm in diameter. No skin burns were noted.

To assess the relative tissue stiffness change during heating, we focus on the oscillatory displacements when heating started [see Fig. 6(a)], i.e., after 0–0.3 s of heating, and after the lesion was formed [see Fig. 6(b)], i.e., after 10.5–10.8 s of heating. These oscillatory displacements are displayed in Fig. 7(a) and (b). After lesion was formed, the relative tissue stiffening was identified by a 30% decrease in displacement amplitude. The change in the displacement amplitude during heating implied that the tissue coagulated [13]. Note that if the reference frame was not at zero, there was an offset in the estimated HMI displacement, as shown in Figs. 5–7. However, this is not a concern in HMI, because the measured peak-to-peak displacement amplitude is independent of this offset. The average peak-to-peak displacement amplitudes from 16 lesions before and after lesion formation were equal to 27.34 ± 1.34 μm and 20.98 ± 1.82 μm, respectively (see Fig. 8). Comparison of displacement amplitude from two cases using a t-test showed a statistically significant difference in HMI displacement before and after lesion formation ($p < 0.001$).

In order to verify the coagulation necrosis, i.e., cell death, in the tumor region, the tumor tissues were excised for subsequent pathology analysis. The histology image of untreated mammary tumor at 100× magnification is shown in Fig. 9(a). The solid tumor nodules are separated by stroma, and each contained densely packed tumor cells (blue–purple) with the white arrows denoting erythrocytes (red blood cells). However, the histology image (H&E stain, original magnification 100×) of the ablated mammary tumors shows that the cells become damaged and necrotic as indicated by hemorrhage [see Fig. 9(b)–white arrows] and fine fibrous strands outlined by adipose tissue (white lobes).

IV. Discussion

The findings presented herein demonstrate the initial results of monitoring thermal ablation, using HMIFU *in vivo*. In this study, we show that HMIFU has the ability to monitor tissue stiffness changes during heating by simultaneously probing and forming lesions at variable depths within the tissue. An amplitude-modulation waveform was used to generate a harmonic radiation force, and as a result the induced tissue motion was also purely harmonic. The tissue mechanical property changes induced by heating were dictated by the induced temperature rise and duration exposure. In other words, when the thermal dose exceeded a certain threshold, irreversible mechanical tissue changes occur and a lesion is formed. Changes in tissue mechanical properties based on the HMI displacement during heating demonstrated that HMIFU could follow the tissue coagulation and thus provide a precise and optimal exposure time (thermal dose).

In this study, for the thermal treatment of tumors *in vivo*, an acoustic intensity (I_{spta}) of 1050 W/cm^2 and duration of exposure of 13.5 s for each location were used to ablate the entire tumor volume. However, the exposure time may vary because it depends on the dimensions and type of tumor being treated. Our preliminary results show that the tumor cells were damaged by the appearance of hemorrhage and necrotic cells in the ablated region in contrast with the nonablated tumor cells (see Fig. 9).

A limitation of this study is the absence of temperature measurement during thermal treatment. The placement of a thermocouple within the tumor will generate additional heat accumulation due to the beam interference with the thermocouple. This would influence the associated displacement estimation. Hence, simultaneous temperature measurement was excluded in this study. However, in previous studies, we have shown good agreement between the HMI displacement profiles and the temperature variation at various exposure durations in bovine liver *in vitro* [13]. Previous work also showed that HMIFU could detect the onset of coagulation necrosis due to an increase in the displacement when the heating was initially applied. In this study, the displacement amplitude did not increase at the exact time the heating started. One possible explanation is the effect of heating on tumor cells and tumor vascular vessels. The tumor tissue is highly vascularized, which might influence the heat distribution and thus the cooling effect from perfusion (blood flow). Ongoing studies include the implementation of a fine-wire thermocouple to enable simultaneous monitoring temperature rise, tumor treatment outcome, and evaluation of the therapeutic efficacy on additional mice.

V. Conclusion

In this study, we demonstrated the HMI feasibility for monitoring FUS ablation *in vivo*. The overlaid color-coded harmonic displacement offers important, complementary information to that of the B-mode or M-mode images. HMI can thus be used as a guidance tool for visualization of the targeted region and monitoring of the relative tissue stiffness changes during heating in real time so that the treatment procedure can be performed in a time-efficient manner. Therefore, HMI can help monitor the lesion formation, control the lesion size, and timely stop the treatment upon lesion formation. HMIFU may thus constitute a cost-efficient and reliable alternative method for real-time monitoring of thermal ablation.

Acknowledgment

The authors would like to thank T. Ludwig and R. Shakya of the Department of Pathology at Columbia University for providing the transgenic mouse model of breast cancer, and J. Luo of the Ultrasound and Elasticity Imaging Laboratory for his kind help.

References

[1] J. E. Kennedy, "High-intensity focused ultrasound in the treatment of solid tumours," *Nat. Rev. Cancer*, vol. 5, pp. 321–327, 2005.

[2] J. Gellermann, W. Wlodarczyk, A. Feussner, H. Fahling, J. Nadobny, B. Hildebrandt, R. Felix, and P. Wust, "Methods and potentials of magnetic resonance imaging for monitoring radio frequency hyperthermia in a hybrid system," *Int. J. Hyperther.*, vol. 21, pp. 497–513, 2005.

[3] H. E. Cline, K. Hynynen, R. D. Watkins, W. J. Adams, J. F. Schenck, R. H. Ettinger, W. R. Freund, J. P. Vetro, and F. A. Jolesz, "Focused US system for MR imaging-guided tumor ablation," *Radiology*, vol. 194, pp. 731–737, 1995.

[4] S. van Esser, M. Van Den Bosch, P. J. van Diest, W. T. M. Mali, I. Rinkes, and R. van Hillegersberg, "Minimally invasive ablative therapies for invasive breast carcinomas: An overview of current literature," *World J. Surg.*, vol. 31, pp. 2284–2292, 2007.

[5] P. E. Huber, J. W. Jenne, R. Rastert, I. Simiantonakis, H. P. Sinn, H. J. Strittmatter, D. von Fournier, M. F. Wannenmacher, and J. Debus, "A new noninvasive approach in breast cancer therapy using magnetic resonance imaging-guided focused ultrasound surgery," *Cancer Res.*, vol. 61, pp. 8441–8447, 2001.

[6] K. Hynynen, O. Pomeroy, D. N. Smith, P. E. Huber, N. J. McDannold, J. Kettenbach, J. Baum, S. Singer, and F. A. Jolesz, "MR imaging-guided focused ultrasound surgery of fibroadenomas in the breast: A feasibility study," *Radiology*, vol. 219, pp. 176–185, 2001.

[7] D. Gianfelice, A. Khiat, M. Amara, A. Belblidia, and Y. Boulanger, "MR imaging-guided focused ultrasound surgery of breast cancer: Correlation of dynamic contrast-enhanced MRI with histopathologic findings," *Breast Cancer Res. Treat.*, vol. 82, pp. 93–101, 2003.

[8] H. Furusawa, K. Namba, S. Thomsen, F. Akiyama, A. Bendet, C. Tanaka, Y. Yasuda, and H. Nakahara, "Magnetic resonance-guided focused ultrasound surgery of breast cancer: Reliability and effectiveness," *J. Amer. Coll. Surg.*, vol. 203, pp. 54–63, 2006.

[9] L. Curiel, R. Chopra, and K. Hynynen, "In vivo monitoring of focused ultrasound surgery using local harmonic motion," *Ultrasound Med. Biol.*, vol. 35, pp. 65–78, 2009.

[10] F. L. Lizzi, R. Muratore, C. X. Deng, J. A. Ketterling, S. K. Alam, S. Mikaelian, and A. Kalisz, "Radiation-force technique to monitor lesions during ultrasonic therapy," *Ultrasound Med. Biol.*, vol. 29, pp. 1593–1605, 2003.

[11] E. E. Konofagou and K. Hynynen, "Localized harmonic motion imaging: Theory, simulations and experiments," *Ultrasound Med. Biol.*, vol. 29, pp. 1405–1413, 2003.

[12] F. S. van Kleef, J. V. Boskamp, and M. Van Den Tempel, "Determination of the number of cross-links in a protein gel from its mechanical and swelling properties," *Biopolymers*, vol. 17, pp. 225–35, 1978.

[13] C. Maleke and E. E. Konofagou, "Harmonic motion imaging for focused ultrasound (HMIFU): A fully integrated technique for sonication and monitoring of thermal ablation in tissues," *Phys. Med. Biol.*, vol. 53, pp. 1773–1793, 2008.

[14] T. Wu, J. P. Felmlee, J. F. Greenleaf, S. J. Riederer, and R. L. Ehman, "Assessment of thermal tissue ablation with MR elastography," *Magn. Reson. Med.*, vol. 45, pp. 80–87, 2001.

[15] C. Maleke, M. Pernot, and E. E. Konofagou, "A Single-element focused ultrasound transducer method for harmonic motion imaging," *Ultrason. Imag.*, vol. 28, pp. 144–158, 2006.

[16] J. Vappou, C. Maleke, and E. E. Konofagou, "Quantitative viscoelastic parameters measured by Harmonic Motion Imaging," *Phys. Med. Biol.*, vol. 54, pp. 3579–3594, 2009.

[17] R. Shakya, M. Szabolcs, E. McCarthy, E. Ospina, K. Basso, S. Nandula, V. Murty, R. Baer, and T. Ludwig, "The basal-like mammary carcinomas induced by Brca1 or Bard1 inactivation implicate the BRCA1/BARD1 heterodimer in tumor suppression," in *Proc. Nat. Acad. Sci. USA*, vol. 105, pp. 7040–7045, 2008.

[18] T. Ludwig, P. Fisher, V. Murty, and A. Efstratiadis, "Development of mammary adenocarcinomas by tissue-specific knockout of Brca2 in mice," *Oncogene*, vol. 20, pp. 3937–3948, 2001.